University of Dundee

A rare missense mutation in GJB3 (Cx31G45E) is associated with a unique cellular phenotype resulting in necrotic cell death

Easton, J. A.; Alboulshi, A. K.; Kamps, M. A. F.; Brouns, G. H.; Broers, M. R.; Coull, B. J.; Oji, V.; van Geel, M.; van Steensel, M. A. M.; Martin, P. E.

DR. PATRICIA E MARTIN (Orcid ID : 0000-0003-0890-8059)

Article type   : Regular Article

A rare missense mutation in *GJB3* (Cx31G45E) is associated with a unique cellular phenotype resulting in necrotic cell death

[#]J.A. Easton[1,2,] [#]A.K. Alboulshi[3], M.A.F. Kamps[1,2], G.H. Brouns [1], M.R. Broers[1], B.J. Coull[4], V. Oji[5], M. van Geel[1,2,5], M.A.M. van Steensel[4,5,6], P.E. Martin[3],

[1]*Department of Dermatology,* [2]*GROW School for Oncology and Developmental Biology, Maastricht University, Maastricht, The Netherlands,* [3]*Department of Life Sciences, School of Health and Life Sciences, Glasgow Caledonian University, Glasgow, UK;* [4]*Division of Biological Chemistry and Drug Discovery, College of Life Sciences, University of Dundee, Dundee, UK,* [5]*Department of Dermatology, University Hospital Münster, Münster, Germany,* [5]*Department of Clinical Genetics, MUMC+, Maastricht, The Netherlands, Division of Cancer Research, School of Medicine,* [6]*Skin Research Institute of Singapore, Institute of Medical Biology, Immunos, Singapore*

[#]JAE and AKA contributed equally to this work and share first authorship

Correspondence to:

[3]Patricia E Martin: email: patricia.martin@gcu.ac.uk

Postal address: Dr P Martin, School of Health and Life Sciences, Department of Life Sciences, Glasgow Caledonian University, Glasgow, G4 0BA, Scotland, UK.

Tel: +44 141 331 3726

Abstract

Erythrokeratodermia variabilis et progressiva (EKV-P) is caused by mutations in either the *GJB3* (Cx31) or *GJB4* gene (Cx30.3). We identified a rare *GJB3* missense mutation, c.134G>A (p.G45E), in two unrelated patients and investigated its cellular characteristics. Expression of Cx31G45E-GFP caused previously undescribed changes within HeLa cells and HaCaT cells, a model human keratinocyte cell line. Cx31WT-GFP localised to the plasma membrane, but expression of Cx31G45E-GFP caused vacuolar expansion of the endoplasmic reticulum (ER), the mutant protein accumulated within the ER membrane and disassembly of the microtubular network occurred. No ER stress responses were evoked. Cx31WT-myc-myc-6xHis and Cx31G45E-GFP co-immunoprecipitated, indicative of heteromeric interaction, but co-expression with Cx31WT-mCherry, Cx26 or Cx30.3 did not mitigate the phenotype. Cx31 and Cx31G45E both co-immunoprecipated with Cx43, indicating the ability to form heteromeric connexons. WT-Cx31 and Cx43 assembled into large gap junction plaques at points of cell to cell contact, Cx31G45E restricted the ability of Cx43 to reach the plasma membrane in both HaCaT cells and HeLa cells stably expressing Cx43 where the proteins strongly co-localised with the vacolourised ER. Cell viability assays identified an increase in cell death in cells expressing Cx31G45E-GFP, which FACS analysis determined was necrotic. Blocking connexin channel function with 18α-Glycyrrhetinic acid did not completely rescue necrosis or prevent propidium iodide uptake, suggesting that expression of Cx31G45E-GFP damages the cellular membrane independent of its channel function. Our data suggests that entrapment of Cx43 and necrotic cell death in the epidermis could underlie the EKV skin phenotype.

1. INTRODUCTION

A healthy skin barrier requires a highly ordered and tightly regulated intercellular adhesion network, which includes adherens junctions, tight junctions and gap junctions (GJ). GJs mediate rapid intercellular communication and play a key role in epidermal integrity [1]. They are composed of connexins (Cxs), with 21 subtypes identified in humans, ranging in size from 25 to 62 kDa, with their nomenclature based on their molecular mass, e.g., Cx31 is a 31kDa protein [2]. Cxs are composed of four transmembrane domains linked by two highly conserved extracellular loops (EL1 and EL2) with one variable intracellular loop and carboxyl tail [3]. Cxs follow a classic biosynthetic pathway from the endoplasmic reticulum (ER), where they oligomerise to form a hexameric connexon (or hemichannel), that is trafficked in a closed state to the plasma membrane. Hemichannels can be induced to open under pathological conditions, but normally accrete laterally in a closed state along the plasma membrane to align and dock with a neighbouring channel and form a functional GJ unit [1, 3]. Within normal epidermis, at least six Cx subtypes are differentially expressed. Connexin43 (encoded by *GJA1*) and Cx31 (encoded by *GJB3*) are expressed throughout the epidermis, while Cx26 (encoded by *GJB2*), Cx30 (encoded by *GJB6*), Cx30.3 (encoded by *GJB4*) tend to be associated with differentiated cells in the upper layers [4-8]. The importance of connexins in the skin is illustrated by various disorders caused by mutations in different beta-Cx subtypes [9-16]. Erythrokeratodermia variabilis et progressiva (EKV-P) (Mendes da Costa, EKV-P, MIM #133200) is caused by heterozygous mutations in either Cx31 or Cx30.3 e.g. [17-25]. The clinical appearance of EKV-P ranges from temporary, fast moving erythemas to permanent red-brown hyperkeratosis (supplementary Table 1). With the possible exception of an erythema gyratum repens-like manifestation of EKV-P caused by Cx30.3 mutations, a genotype-phenotype correlation is not present [20, 26]. Disease-associated Cx31 mutations, when expressed in HeLa cells, result in both apoptotic and necrotic cell death [27, 28]. Several studies indicate that ER stress is involved in this process [27, 29, 30]. We describe how a rare EKV-associated Cx31 mutant (G45E) [20, 22, 24] causes necrotic cell death through a unique effect on the ER and entrapment of Cx43. We suggest that this may be a novel connexin-mediated human disease mechanism.

2. MATERIALS AND METHODS

2.1 Construction of tagged Cx-WT and mutant constructs

Wild type (WT) Cx31 was inserted into the vector pEGFP-N1 (BD Biosciences, Breda, The Netherlands) as previously reported and a range of mutations (Cx31G45E, Cx31delG45, Cx31G45A,

Cx31G45K, Cx31G45S, Cx31G45Q and Cx31G45W) introduced by site directed mutagenesis (see supplementary methods and supplementary Table 2) [12]. Cx31WT, Cx26WT and Cx30.3WT were inserted into the pmCherry-N1 vector (Clontech, via Westburg BV, Leusden, The Netherlands). A two-step process replacing the GFP tag with a myc-myc-6xHis tag from a plasmid gifted from Thomas Weimbs (Addgene plasmid # 12377 [31]) was used to generate a Cx31WT-myc-myc-6xHis tagged construct.

2.2 Cell Culture and transfection

Cell lines, HeLa Ohio (ATTC) and HaCaT cells (CLS, Eppelheim, Germany) or HeLa cells stably expressing Cx43 or Cx26 [32] were cultured under optimal conditions (see supplementary methods) and were transfected with relevant plasmid DNA for 24 h. Transfection efficiency was 30-50%, assessed by GFP or mCherry auto fluorescence.

Cells were treated as required with the Cx channel blocker 18α glycyrrhetinic acid (18αGA) (25μM, Sigma) for the duration of the experiment. Thapsigargin (1μM, Sigma) was added for 8h prior to RNA and protein extraction to induce ER stress where appropriate.

2.3 Immunofluorescence

Cells were fixed in either ice-cold methanol or 4% (w/v) paraformaldehyde (as per antibody requirements) and processed for immunocytochemical analysis as previously described using a panel of antibodies (see supplementary information) [33].

mCherry or GFP autoflourescence determined localisation of Cx-tagged proteins. Imaging was carried out using a Leica TCS SPE confocal laser scanning fluorescence microscope (Leica DMRBE, Mannheim, Germany) or a Zeiss Axiovert microscope linked up to an 800 Airyscan confocal system. Images were acquired under similar conditions and magnifications and were processed with ImageJ software, version 1.43 (http://rsbweb.nih.gov/ij/) and Adobe Photoshop.

2.4 Protein interactions

HeLa cells selected to stably express Cx31WT-GFP (HeLa31-GFP cells) were transfected with either Cx31WT or Cx31G45E tagged to myc-myc-6xHis. The expression vector eGFP-N1 and a control myc-tagged expression vector were transfected as a positive control for the Western blots. Transfected cells were harvested in NP40 lysis buffer (150mM NaCl, 250mM Tris-HCl (pH 7.3) and 1% (v/v) NP40). To 50µl His Mag Sepharose Ni beads (GE Healthcare Life Sciences, Diegem, Belgium) 500µg total protein was added. The bead and protein mix was incubated at 4°C overnight with agitation. Non-bound protein was removed by washing (250 mM NaCl, 250 mM Tris-HCl, 5 mM Imidazol, 0.1 % (v/v) NP40), followed by elution of bound protein in elution buffer (500 mM NaCl, 250 mM Tris-HCl, 500 mM Imidazol and 0.1% (v/v) NP40).

HeLa43 cells were also transfected with either Cx31WT or Cx31G45E tagged to GFP and were harvested in RIPA buffer (125 mM NaCl, 5 mM EDTA, 1% (w/v) Sodium Deoxycholate and 0.5% (v/v) Triton X-100). Twenty-five µl of sheep anti-rabbit IgG Dynabeads (Thermofisher scientific, UK), previously incubated with polyclonal rabbit - GFP antibody (1:100, Abcam, UK), was then added to 500 μ g of total protein and incubated at 4°C overnight with agitation. The beads were extensively washed to remove any non-specifically bound proteins and interacting proteins finally eluted in 5x Laemmli buffer following manufactures instructions.

2.5 Western blotting

Protein (30 µg) was subjected to SDS-PAGE, and Western blot analysis was performed according to standard procedures and blots were probed with appropriate antibodies (please see supplementary information).

2.6 Quantitative Reverse-transcriptase PCR (qRT-PCR)

Total RNA was isolated from transfected HeLa cells using ISOLATE II RNA Mini Kit according to manufacturers' instructions (Bioline) and cDNA synthesised with the M-MLV reverse transcription kit (Promega, Southhampton, UK). Primers against *CHOP, GADD34* and the reference gene *GAPDH* were used in Taqman PCR reactions (Primer design). The reaction was performed in a Applied Biosystems ViiA™7 Real time PCR system under the following cycling conditions: 95°C for 15 min, followed by 40 cycles of 95°C for 15 s and 60°C for 30 s. Gene expression levels were obtained from the value of

threshold cycle (Ct) for each specific gene and normalised against the Ct of GAPDH ($\Delta\Delta C_T$ method) [34].

2.7 Propidium Iodide (PI) uptake assays and FACS analysis

Transfected cells were pre-treated with 18αGA as required prior to trypsinisation and resuspension in PBS for analysis using a BD FACSCantoII. For each population 20,000 events were gated. To ensure only transfected (GFP expressing) cells were counted, cells were gated to FITC using a 488nm laser. Fluorescence was detected using a 530/30 fluorochrome set at 400V. Forward and side scatter were detected at 340V and 450V respectively. For PI uptake assays the cells were prepared as above then incubated with 40μg/ml PI for 1h, on ice, prior to analysis. PI was detected using a 575/26 fluorochrome set at 300V, in the 488nM gated cells. A control necrotic cell population was prepared by freeze-thawing cells three times prior to analysis. Analysis was carried out using Flowing Software (http://www.flowingsoftware.com, v2.5.1).

2.8 Statistical Analysis

Experiments were performed in triplicate and compiled using GraphPad Prism6 software. Results are expressed as mean ± S.E.M and statistical analysis performed using unpaired t-test, and Dunnett's multiple comparison test as appropriate. ** $P<0.05$; ***$P<0.001$.

RESULTS

3.1 Expression of the mutation Cx31G45E causes a unique cellular morphology *in vitro* and impacts intracellular components

Cx31WT-GFP trafficked to the plasma membrane and assembled into typical gap junction plaque-like structures in HeLa Ohio cells (Figure 1A). In contrast, Cx31G45E-GFP accumulated within the cytoplasm in pronounced vacuole-like structures (Figure 1B). Co-staining with an antibody against SERCA2b (sarcoplasmic reticulum calcium ATPase) showed a diffuse ER distribution in all non-transfected cells and in cells transfected to express Cx31WT-GFP (Figure 1A and B and supplementary Figure 1). By contrast, in Cx31G45E-GFP expressing HeLa cells, SERCA2b co-localised with the mutant protein suggesting that the vacuoles are formed from the ER (Figure 1B). The microtubule network (Figure 1D) was disrupted in cells expressing Cx31G45E, with evidence of

microtubule collapse and bundling in the periphery of the cell in contrast to the stable microtubule network in Cx31WT-GFP cells (Figure 1C and 1D (red cells only)). However, the nuclear pore complex (Figure 1E and F) and nuclear envelope (Supplementary Figure 2U-X and Y-BB) were not affected by expression of Cx31G45E. Other intracellular organelles were also disrupted including the ERGIC, Golgi apparatus and proteasomes, all key waystations in the Cx life cycle (Supplementary Figure 2E-T).

To determine whether the observed Cx31G45E phenotype was mutation- or residue- specific, a number of different mutations were introduced to residue 45 (summarised in Table 1, supplementary data). Glycine was either deleted (delG45, Supplementary Figure 3C), replaced with alanine (G45A, Supplementary Figure 3D), lysine (G45K, Supplementary Figure 3E), glutamine (G45Q, Supplementary Figure 3F), serine (G45S, Supplementary Figure 3G), or tryptophan (G45W, Supplementary Figure 3H). Each mutation caused the same morphological change as observed in cells expressing Cx31G45E; however, in the case of G45A and G45K the effect was less pronounced and clear gap junction plaques were visible.

3.2 Cx31G45E impacts on the spatial localisation of Cx43 and is a dominant mutation

Cx31 mutations associated with EKV are reported to be dominant-negative. We assessed the impact of the mutant Cx31 protein on the intracellular localisation of wild-type connexins expressed in the epidermis. Co-transfection of HeLa cells with Cx31G45E-GFP and Cx31WT-mCherry (Figure 2A) and Cx30.3 (Figure 2B) resulted in co-localisation of the wild type protein and Cx31G45E in gap junction-like plaque structures, however, the wild-type protein was also held in vesicular structures within the cytoplasm (Figure 2A and B). The impact of Cx31G45E on the spatial localisation of Cx26 and Cx43 was also assessed in HeLa cells stably expressing Cx43 or Cx26. Wild-type Cx31 co-localised at the plasma membrane in gap junction plaques with both Cx43 and Cx26 (Supplementary Figure 4A and B). In HeLa26 cells transfected with Cx31G45E the mutant protein still accumulated in vacuoles and perinuclear regions, however punctate staining of Cx26 at the plasma membrane was evident (Figure 2C). By contrast, in HeLa43 cells Cx43 co-localised extensively with the Cx31G45E in the vacuolated ER, with limited localisation at the plasma membrane (Figure 2D). This coincided with the collapse of the microtubule network in Cx31G45E expressing cells. Cx31G45E produced a similar phenotype in keratinocytes where it was trapped in perinuclear regions and in vacuole-like structures and co-localised with Cx43, furthermore, the localisation of Cx43 at the plasma membrane was markedly reduced. (Figure 2E and F). Wild-type Cx31GFP co-localised extensively

with endogenously expressed Cx43, both in intracellular stores, typically around the ERGIC region of the cell and in gap junction plaques. Thus the wild-type proteins did not rescue the accumulation of Cx31G45E in vesicular structures within the cytoplasm, and there was reduced formation of GJ plaques by the wild-type proteins, suggesting that Cx31G45E has a dominant effect. This was most evident for Cx43.

3.3 Formation of heteromeric Connexons

To confirm that the observed co-localisation of Cx31G45E with wild-type Cx31 and Cx43 represented protein-protein interactions, nickel pull-down and immunoprecipitation assays were performed. HeLa cells transfected to express Cx31WT- and Cx31G45E- GFP-tagged proteins expressed a protein of 57kD, while myc-myc-6xHis-tagged proteins were ~33kDa (Figure 3A, con+31myc, con+GFP+31myc and H31-GFP input lanes). Nickel pull-down assays determined that Cx31WT-GFP interacted with Cx31WT-myc-myc-6xHis, as well as with Cx31G45E-myc-myc-6xHis (Figure 3A, H31-GFP +31-myc and H31-GFP + G45E-myc lanes respectively). Thus Cx31G45E forms channels with Cx31WT.

To further probe Cx31 interactions with epidermal connexins we also performed immunoprecipitation assays to study the interaction of Cx31 and Cx31G45E with Cx43. These experiments were performed in HeLa cells stably expressing Cx43 (Figure 3B). The IgG beads were coated with a GFP antibody enabling co-immunoprecipitation with proteins associating with the GFP tagged connexin. Western blot analysis of the co-IP assays detected eGFP (28kD) from control HeLa cells transfected to express eGFP. In HeLa43 cells transfected to express the Cx31-GFP constructs a band of ~57kD, representative of the Cx31-GFP protein was detected (Figure 3 B, IP: GFP). The blot was also probed for Cx43. In the case of the HeLa cells transfected to express eGFP no Cx43 was detected. By contrast, for HeLa43 cells transfected with wild-type or mutant Cx31, Cx43 co-immunoprecipitated with the Cx31 constructs (Figure 3B, IP: Cx43). These results indicate that Cx31 and Cx31- G45E can co-oligomerise with Cx43.

3.4 Cx31G45E expression is associated with necrotic cell death but does not induce ER stress

Previous reports suggest Cx31-EKV associated mutations induce ER stress [27, 29, 30]. Real–time RT-PCR determined that there was no significant increase in the expression of *CHOP/BiP* or *GADD34,* genes associated with UPR and ER stress in HeLa cells expressing either pEGFP-N1, Cx31WT-GFP or

Cx31G45E-GFP (Figure 4A). By contrast, thapsigargin, a known ER stress inducer, significantly induced expression of *CHOP* by 4.7 ±0.8 fold and *GADD34* by 7.2 ± 0.9 fold (P<0.001). Western blot analysis revealed no change in the level of expression of BiP in HeLa cells (Figure 4B) and in HaCaT cells no changes in the level of BiP or GADD34 were observed (Figure 4C). These observations suggest that expression of Cx31G45E-GFP does not induce ER stress, and other factors must be driving the observed ER changes and the localisation of the mutant protein.

Finally, to determine if the gross changes occurring in cellular integrity in cells expressing Cx31G45E were associated with apoptosis or necrosis, FACS analysis and propidium iodide (PI) uptake assays in the presence or absence of 18αGA, a connexin channel blocker, were performed (Figure 4D and Supplementary Figure 5). Cells were subjected to FACS analysis and under non-transfected control conditions, ~4% of the population exhibited a necrotic profile compared to ~70% of cells from the induced necrotic population (Figure 4D and supplementary Figure 5). Using the FACS parameters established in control conditions, ~6% of cells transfected with pEGFP-N1 and ~4% of cells transfected to express Cx31WT-GFP were detected in the necrotic quadrant (Figure 4E). By contrast, ~25% of cells expressing Cx31-G45E-GFP were necrotic and the effect was not significantly reduced by co-treatment with 18αGA to block hemichannel activity (Figure 4E). Thus the Cx31G45E expressing cells showed a statistically significant (p<0.05) necrotic profile compared to cells expressing wildtype Cx31. Integrity of the cell membrane was also examined via PI uptake assays. Under non-transfected conditions, cells subject to necrosis exhibited a $PI_{(bright)}$ peak that was absent in the control population. In gated, GFP expressing cells a $PI_{(bright)}$ peak was also observed in cells expressing Cx31G45E-GFP, but was absent from cells expressing Cx31WT-GFP or pEGFP-N1. This $PI_{(bright)}$ peak was marginally, but not significantly reduced in the Cx31G45E-GFP populations treated with 18αGA. This suggests that the observed permeability to PI is not due to 'leaky connexin channels' and that the Cx31G45E cells have a compromised membrane (Supplementary Figure 6).

3. Discussion

The present work details the importance of the amino acid position G45 in Cx31 in maintaining cell function and suggests that altered interaction with Cx43 is associated with the pathology of EKV-P. Cx mutations associated with skin disease can alter the connexin life cycle in two primary ways. Firstly, mutations modify trafficking to the plasma membrane. For example, the EKV-P associated mutations G12R, G12D and F137L cause the connexins to be sequestered within the cytoplasm, with loss of channel function [35-37]. Secondly, mutant proteins target the plasma membrane but form 'leaky hemichannels' commonly considered as gain-of-function mutations. This includes a variety of

Cx26 mutations, including Cx26G45E, associated with the inflammatory skin disease Keratitis Ichthyosis Deafness syndrome (KID) [38, 39].

Mutations introduced to Cx31G45 cause a unique phenotype, with the mutant protein sequestered within the ER in vesicular structures. All the EKV mutations reported to date cause abnormal Cx31 trafficking with the mutant proteins accumulating in intracellular stores, particularly the ER [27-29, 36, 38-40] (summarised in supplementary Table 1). This is the first report of extensive disruption of the ER and microtubule network subsequent to a Cx31 mutation. A number of trafficking mutations are also associated with Cx26, with the mutant protein trapped in the ER/Golgi environs, e.g. D66H associated with Vohwinkel syndrome and H73R associated with palmoplantar keratoderma [10, 12]. A recent report suggests that the H73R mutation may interact with Cx43 channels, inducing changes in the functional status of Cx43 [41]. Other mutations in Cx26, primarily associated with the amino terminal domain and the first part of first extracellular loop, are linked with KID syndrome. Recent studies indicate that a variety of Cx26 mutations have trans-dominant effects on other epidermal connexins, including Cx43, inducing altered heteromeric channel function [41-43].

Connexin 31 is expressed in the skin with a similar profile to that of Cx43 [44]. Previous studies have suggested that Cx31 and Cx43 do not form functional heteromeric channels [45]. However, an ability of these channels to functionally interact has been hinted at in a number of studies. In the skin of Cx43 deficient mice, Cx31 was significantly down-regulated and associated with enhanced rates of wound closure [44]. A EKV-mouse model for the mutation Cx31F137L revealed that homozygous mice were non-viable, but that the heterozygous mice had similar wound healing capacities to the Cx43 conditional knockout mice, suggesting functional interactions between these two proteins [23]. In the present work, we observed that Cx43 and Cx31 strongly co-localised at regions of cell to cell contact in both HeLa43 cells and HaCaT cells. Immunoprecipitation assays confirmed the interaction of these two proteins. In both HeLa43 and HaCaT cells expressing the Cx31G45E mutation Cx43 co-localised with the mutation, being trapped inside the cell in the associated G45E-like vacuoles, suggesting a trans-dominant effect. Rapid remodelling and turnover of Cx43/Cx31 proteins and differing levels of heteromeric interaction could account for altered cellular signalling and the transient keratosis and erythema associated with EKV, although such speculations require further analysis.

The effect of Cx31G45E expression *in vitro* was very different to that reported for Cx26G45E and other non-trafficking mutations in Cx31 and Cx26, with pronounced disruption of the ER. The amino acid G45, located on the first extracellular loop of connexins, is highly conserved among all Cx subtypes. Structural analysis for Cx26 revealed the importance of G45 in lining the extracellular

funnel, suggesting that this amino acid is critical for channel function [46]. Zhang *et al.* examined the G45E mutation in Cxs30, 32 and 43 and showed that cell death occurred within 24 h of transfection, which could be rescued by incubating cells in >5 mM Ca^{2+} [47], suggesting that G45 is a common calcium sensing centre for connexins. Each of the amino acid substitutions in the present study introduced subtle changes to properties at this position. While G45E introduces an acidic residue, G45K and G45S mutations result in a change in charge to positive and neutral amino acids respectively. The G45K mutation induced a negative to positive charge while introduction of glutamine results in a change in the size of the amino acid and introducing tryptophan (G45W) causes a switch from a hydrophilic to a hydrophobic amino acid. All these amino acid changes, including deletion of G45, deregulated Cx31 transport. By contrast, Zhang *et al*. showed that a G45E mutation in Cxs43 and 32 had no effect on protein trafficking. Although the mutation Cx26G45E is associated with a lethal form of KID, little alteration in spatial localisation of the protein has been reported, however leaky hemichannels form that are extremely sensitive to changes in calcium levels [48, 49]. Thus our data clearly illustrates the importance of the glycine at position 45 in maintaining Cx31 structure.

Connexin trafficking relies on an intact microtubule network, with plus end tracking motor proteins and partners such as consortin required for efficient membrane delivery [50, 51]. We observed a profound re-localisation of Cx43 with Cx31G45E, suggesting a trans-dominant effect on Cx43 trafficking. It is well established that Cx43 trafficking is highly dependent on an intact microtubular network and further studies are now required to determine how heteromeric mutant channels may interact with transport networks [50, 51] .

ER stress and an unfolded protein response (UPR) have been reported in several EKV-P mutations and are key events in inducing necrotic cell death [27-29, 36, 40]. Although our studies showed no evidence of ER stress, FACS analysis and PI uptake assays determined that the mutation induced necrotic cell death, an endpoint also observed for the other EKV-P mutations and highly likely linked to altered keratinization [52]. The lack of ER stress could be attributed to a breakdown of the microtubule network, required for maintaining ER structure [53], suggesting this may be an early event following expression of the mutant protein.

Our observations suggest that diverse, mutation-specific mechanisms lead to necrotic cell death associated with the EKV-P phenotype. In cells expressing the mutation Cx31R42P, induced ER stress promoted production of reactive oxygen species (ROS), which stimulated hemichannel activity and promoted cell death [27]. Hemichannel blockers or high extracellular calcium decreased the level of cell death. Interestingly, the cell death phenotype was promoted when the cells were grown at low

temperature (26°C). Tang and colleagues [28] reported that the trafficking deficiency and loss of function of mutations Cx31-G12D, R42P and F137L was recovered by culturing cells at 27°C. These authors also reported that BiP/Hsp70 and cFos-JunB pathways are central in EKV. A further Cx31 mutation V174M, associated with non-syndromic deafness but with no skin pathology reported, accumulated in lysosomes and the ER [54]. This mutation also formed non-functional channels and had a trans-dominant effect on the trafficking of Cx26 but did not alter the ability of WTCx31 to assemble at the plasma membrane.

In conclusion, four clinical reports indicate that G45E is associated with EKV-P. To our knowledge, our report is the first to detail the impact of this mutation on cellular integrity and provides evidence that disease progression is associated with necrotic cell death. We also show that the mutation has a trans-dominant effect on the trafficking of Cx43 which, together with recent data for Cx26 [42, 43], suggest altered interaction with Cx43 may be indicative of severe Cx-related skin disorders. Although the EKV-P phenotype associated with this mutation is similar to other EKV-P mutations reported it is clear that the underlying mechanism attributed to the mutation is different, suggesting variable mechanisms of triggering the disease state and warrants further investigation.

Conflict of Interest: None to declare

References

1. Martin, P. E.; Easton, J. A.; Hodgins, M. B.; Wright, C. S., Connexins: sensors of epidermal integrity that are therapeutic targets. *FEBS Lett* **2014,** 588, (8), 1304.
2. Willecke, K.; Eiberger, J.; Degen, J.; Eckardt, D.; Romualdi, A.; Guldenagel, M.; Deutsch, U.; Sohl, G., Structural and functional diversity of connexin genes in the mouse and human genome. *Biol Chem* **2002,** 383, (5), 725.
3. Laird, D. W., Life cycle of connexins in health and disease. *Biochem J* **2006,** 394, (Pt 3), 527.
4. Di, W. L.; Rugg, E. L.; Leigh, I. M.; Kelsell, D. P., Multiple epidermal connexins are expressed in different keratinocyte subpopulations including connexin 31. *J Invest Dermatol* **2001,** 117, (4), 958.

5.   Kandyba, E. E.; Hodgins, M. B.; Martin, P. E., A murine living skin equivalent amenable to live-cell imaging: analysis of the roles of connexins in the epidermis. *J Invest Dermatol* **2008,** 128, (4), 1039.

6.   Kretz, M.; Maass, K.; Willecke, K., Expression and function of connexins in the epidermis, analyzed with transgenic mouse mutants. *Eur J Cell Biol* **2004,** 83, (11-12), 647.

7.   Wiszniewski, L.; Limat, A.; Saurat, J. H.; Meda, P.; Salomon, D., Differential expression of connexins during stratification of human keratinocytes. *J Invest Dermatol* **2000,** 115, (2), 278.

8.   Maher, A. C.; Thomas, T.; Riley, J. L.; Veitch, G.; Shao, Q.; Laird, D. W., Rat epidermal keratinocytes as an organotypic model for examining the role of Cx43 and Cx26 in skin differentiation. *Cell Commun Adhes* **2005,** 12, (5-6), 219.

9.   Abrams, C. K.; Freidin, M.; Bukauskas, F.; Dobrenis, K.; Bargiello, T. A.; Verselis, V. K.; Bennett, M. V.; Chen, L.; Sahenk, Z., Pathogenesis of X-linked Charcot-Marie-Tooth disease: differential effects of two mutations in connexin 32. *J Neurosci* **2003,** 23, (33), 10548.

10.   Bakirtzis, G.; Choudhry, R.; Aasen, T.; Shore, L.; Brown, K.; Bryson, S.; Forrow, S.; Tetley, L.; Finbow, M.; Greenhalgh, D.; Hodgins, M., Targeted epidermal expression of mutant Connexin 26(D66H) mimics true Vohwinkel syndrome and provides a model for the pathogenesis of dominant connexin disorders. *Hum Mol Genet* **2003,** 12, (14), 1737.

11.   Common, J. E.; Becker, D.; Di, W. L.; Leigh, I. M.; O'Toole, E. A.; Kelsell, D. P., Functional studies of human skin disease- and deafness-associated connexin 30 mutations. *Biochem Biophys Res Commun* **2002,** 298, (5), 651.

12.   de Zwart-Storm, E. A.; Hamm, H.; Stoevesandt, J.; Steijlen, P. M.; Martin, P. E.; van Geel, M.; van Steensel, M. A., A novel missense mutation in GJB2 disturbs gap junction protein transport and causes focal palmoplantar keratoderma with deafness. *J Med Genet* **2008,** 45, (3), 161.

13.   Debeer, P.; Van Esch, H.; Huysmans, C.; Pijkels, E.; De Smet, L.; Van de Ven, W.; Devriendt, K.; Fryns, J. P., Novel GJA1 mutations in patients with oculo-dento-digital dysplasia (ODDD). *Eur J Med Genet* **2005,** 48, (4), 377.

14.   Diestel, S.; Richard, G.; Doring, B.; Traub, O., Expression of a connexin31 mutation causing erythrokeratodermia variabilis is lethal for HeLa cells. *Biochem Biophys Res Commun* **2002,** 296, (3), 721.

15.   Garcia, I. E.; Maripillan, J.; Jara, O.; Ceriani, R.; Palacios-Munoz, A.; Ramachandran, J.; Olivero, P.; Perez-Acle, T.; Gonzalez, C.; Saez, J. C.; Contreras, J. E.; Martinez, A. D., Keratitis-ichthyosis-deafness syndrome-associated cx26 mutants produce nonfunctional gap junctions but hyperactive hemichannels when co-expressed with wild type cx43. *J Invest Dermatol* **2015,** 135, (5), 1338.

16.   Jonard, L.; Feldmann, D.; Parsy, C.; Freitag, S.; Sinico, M.; Koval, C.; Grati, M.; Couderc, R.; Denoyelle, F.; Bodemer, C.; Marlin, S.; Hadj-Rabia, S., A familial case of Keratitis-Ichthyosis-Deafness (KID) syndrome with the GJB2 mutation G45E. *Eur J Med Genet* **2008,** 51, (1), 35.

17.   Common, J. E.; O'Toole, E. A.; Leigh, I. M.; Thomas, A.; Griffiths, W. A.; Venning, V.; Grabczynska, S.; Peris, Z.; Kansky, A.; Kelsell, D. P., Clinical and genetic heterogeneity of erythrokeratoderma variabilis. *J Invest Dermatol* **2005,** 125, (5), 920.

18.   Feldmeyer, L.; Plantard, L.; Mevorah, B.; Huber, M.; Hohl, D., Novel mutation of connexin 31 causing erythrokeratoderma variabilis. *Br J Dermatol* **2005,** 152, (5), 1072.

19.   Fuchs-Telem, D.; Pessach, Y.; Mevorah, B.; Shirazi, I.; Sarig, O.; Sprecher, E., Erythrokeratoderma variabilis caused by a recessive mutation in GJB3. *Clin Exp Dermatol* **2011,** 36, (4), 406.

20.   Glatz, M.; van Steensel, M. A.; van Geel, M.; Steijlen, P. M.; Wolf, P., An unusual missense mutation in the GJB3 gene resulting in severe erythrokeratodermia variabilis. *Acta Derm Venereol* **2011,** 91, (6), 714.

21.   Morley, S. M.; White, M. I.; Rogers, M.; Wasserman, D.; Ratajczak, P.; McLean, W. H.; Richard, G., A new, recurrent mutation of GJB3 (Cx31) in erythrokeratodermia variabilis. *Br J Dermatol* **2005,** 152, (6), 1143.

22.   Renner, R.; Paasch, U.; Simon, J. C.; Froster, U. G.; Heinritz, W., A new mutation in the GJB3 gene in a patient with erythrokeratodermia variabilis. *J Eur Acad Dermatol Venereol* **2008,** 22, (6), 750.

23.   Schnichels, M.; Worsdorfer, P.; Dobrowolski, R.; Markopoulos, C.; Kretz, M.; Schwarz, G.; Winterhager, E.; Willecke, K., The connexin31 F137L mutant mouse as a model for the human skin disease erythrokeratodermia variabilis (EKV). *Hum Mol Genet* **2007,** 16, (10), 1216.

24.   Takeichi, T.; Sugiura, K.; Hsu, C. K.; Nomura, T.; Takama, H.; Simpson, M. A.; Shimizu, H.; McGrath, J. A.; Akiyama, M., Erythrokeratoderma Variabilis Caused by p.Gly45Glu in Connexin 31: Importance of the First Extracellular Loop Glycine Residue for Gap Junction Function. *Acta Derm Venereol* **2016,** 96, (4), 557.

25.   Tamaki, Y.; Tamaki, E.; Sakai, R.; Takahashi, K.; Horiguchi, Y., A case of erythrokeratoderma variabilis: loosened gap junctions in the acanthotic epidermis. *J Dermatol* **2006,** 33, (6), 419.

26.   Sbidian, E.; Bousseloua, N.; Jonard, L.; Leclerc-Mercier, S.; Bodemer, C.; Hadj-Rabia, S., Novel Mutation in GJB4 Gene (Connexin 30.3) in a Family with Erythrokeratodermia Variabilis. *Acta Derm Venereol* **2013,** 93, (2), 193.

27.   Chi, J.; Li, L.; Liu, M.; Tan, J.; Tang, C.; Pan, Q.; Wang, D.; Zhang, Z., Pathogenic connexin-31 forms constitutively active hemichannels to promote necrotic cell death. *PLoS One* **2012,** 7, (2), e32531.

28.   Tang, C.; Chen, X.; Chi, J.; Yang, D.; Liu, S.; Liu, M.; Pan, Q.; Fan, J.; Wang, D.; Zhang, Z., Pathogenic Cx31 is un/misfolded to cause skin abnormality via a Fos/JunB-mediated mechanism. *Hum Mol Genet* **2015,** 24, (21), 6054.

29.   Tattersall, D.; Scott, C. A.; Gray, C.; Zicha, D.; Kelsell, D. P., EKV mutant connexin 31 associated cell death is mediated by ER stress. *Hum Mol Genet* **2009,** 18, (24), 4734.

30.   Xia, K.; Ma, H.; Xiong, H.; Pan, Q.; Huang, L.; Wang, D.; Zhang, Z., Trafficking abnormality and ER stress underlie functional deficiency of hearing impairment-associated connexin-31 mutants. *Protein Cell* **2010,** 1, (10), 935.

31.   Low, S. H.; Vasanji, A.; Nanduri, J.; He, M.; Sharma, N.; Koo, M.; Drazba, J.; Weimbs, T., Syntaxins 3 and 4 are concentrated in separate clusters on the plasma membrane before the establishment of cell polarity. *Mol Biol Cell* **2006,** 17, (2), 977.

32.   Wright, C. S.; van Steensel, M. A.; Hodgins, M. B.; Martin, P. E., Connexin mimetic peptides improve cell migration rates of human epidermal keratinocytes and dermal fibroblasts in vitro. *Wound Repair Regen* **2009,** 17, (2), 240.

33.   Martin, P. E.; Wall, C.; Griffith, T. M., Effects of connexin-mimetic peptides on gap junction functionality and connexin expression in cultured vascular cells. *Br J Pharmacol* **2005,** 144, (5), 617.

34.   Donnelly, S.; English, G.; de Zwart-Storm, E. A.; Lang, S.; van Steensel, M. A.; Martin, P. E., Differential susceptibility of Cx26 mutations associated with epidermal dysplasias to peptidoglycan derived from Staphylococcus aureus and Staphylococcus epidermidis. *Exp Dermatol* **2012,** 21, (8), 592.

35.   Di, W. L.; Monypenny, J.; Common, J. E.; Kennedy, C. T.; Holland, K. A.; Leigh, I. M.; Rugg, E. L.; Zicha, D.; Kelsell, D. P., Defective trafficking and cell death is characteristic of skin disease-associated connexin 31 mutations. *Hum Mol Genet* **2002,** 11, (17), 2005.

36.   He, L. Q.; Liu, Y.; Cai, F.; Tan, Z. P.; Pan, Q.; Liang, D. S.; Long, Z. G.; Wu, L. Q.; Huang, L. Q.; Dai, H. P.; Xia, K.; Xia, J. H.; Zhang, Z. H., Intracellular distribution, assembly and effect of disease-associated connexin 31 mutants in HeLa cells. *Acta Biochim Biophys Sin (Shanghai)* **2005,** 37, (8), 547.

37.   Yoshikata-Isokawa, Y.; Itoh, M.; Nakagawa, H., Japanese sporadic case of erythrokeratodermia variabilis caused by the connexin-30.3 (GJB4) mutation: Is Glycine 12 a mutational hotspot in the connexin family? *J Dermatol* **2016**.

38.   Gerido, D. A.; DeRosa, A. M.; Richard, G.; White, T. W., Aberrant hemichannel properties of Cx26 mutations causing skin disease and deafness. *Am J Physiol Cell Physiol* **2007,** 293, (1), C337.

39.   Martin, P. E.; van Steensel, M., Connexins and skin disease: insights into the role of beta

connexins in skin homeostasis. *Cell Tissue Res* **2015,** 360, (3), 645.

40.   Scott, C. A.; O'Toole, E. A.; Mohungoo, M. J.; Messenger, A.; Kelsell, D. P., Novel and recurrent connexin 30.3 and connexin 31 mutations associated with erythrokeratoderma variabilis. *Clin Exp Dermatol* **2011,** 36, (1), 88.

41.   Shuja, Z.; Li, L.; Gupta, S.; Mese, G.; White, T. W., Connexin26 Mutations Causing Palmoplantar Keratoderma and Deafness Interact with Connexin43, Modifying Gap Junction and Hemichannel Properties. *J Invest Dermatol* **2016,** 136, (1), 225.

42.   Garcia, I. E.; Bosen, F.; Mujica, P.; Pupo, A.; Flores-Munoz, C.; Jara, O.; Gonzalez, C.; Willecke, K.; Martinez, A. D., From Hyperactive Connexin26 Hemichannels to Impairments in Epidermal Calcium Gradient and Permeability Barrier in the Keratitis-Ichthyosis-Deafness Syndrome. *J Invest Dermatol* **2016,** 136, (3), 574.

43.   Press, E. R.; Shao, Q.; Kelly, J. J.; Chin, K.; Alaga, A.; Laird, D. W., Induction of cell death and gain-of-function properties of connexin26 mutants predict severity of skin disorders and hearing loss. *J Biol Chem* **2017,** 292, (23), 9721.

44.   Kretz, M.; Euwens, C.; Hombach, S.; Eckardt, D.; Teubner, B.; Traub, O.; Willecke, K.; Ott, T., Altered connexin expression and wound healing in the epidermis of connexin-deficient mice. *J Cell Sci* **2003,** 116, (Pt 16), 3443.

45.   Elfgang, C.; Eckert, R.; Lichtenberg-Frate, H.; Butterweck, A.; Traub, O.; Klein, R. A.; Hulser, D. F.; Willecke, K., Specific permeability and selective formation of gap junction channels in connexin-transfected HeLa cells. *J Cell Biol* **1995,** 129, (3), 805.

46.   Maeda, S.; Nakagawa, S.; Suga, M.; Yamashita, E.; Oshima, A.; Fujiyoshi, Y.; Tsukihara, T., Structure of the connexin 26 gap junction channel at 3.5 A resolution. *Nature* **2009,** 458, (7238), 597.

47.   Zhang, Y.; Hao, H., Conserved glycine at position 45 of major cochlear connexins constitutes a vital component of the Ca(2)(+) sensor for gating of gap junction hemichannels. *Biochem Biophys Res Commun* **2013,** 436, (3), 424.

48.   Sanchez, H. A.; Mese, G.; Srinivas, M.; White, T. W.; Verselis, V. K., Differentially altered Ca2+ regulation and Ca2+ permeability in Cx26 hemichannels formed by the A40V and G45E mutations that cause keratitis ichthyosis deafness syndrome. *J Gen Physiol* **2010,** 136, (1), 47.

49.   Sanchez, H. A.; Verselis, V. K., Aberrant Cx26 hemichannels and keratitis-ichthyosis-deafness syndrome: insights into syndromic hearing loss. *Front Cell Neurosci* **2014,** 8, 354.

50.   Martin, P. E.; Blundell, G.; Ahmad, S.; Errington, R. J.; Evans, W. H., Multiple pathways in the trafficking and assembly of connexin 26, 32 and 43 into gap junction intercellular communication channels. *J Cell Sci* **2001,** 114, (Pt 21), 3845.

51.   Shaw, R. M.; Fay, A. J.; Puthenveedu, M. A.; von Zastrow, M.; Jan, Y. N.; Jan, L. Y., Microtubule plus-end-tracking proteins target gap junctions directly from the cell interior to adherens junctions. *Cell* **2007,** 128, (3), 547.
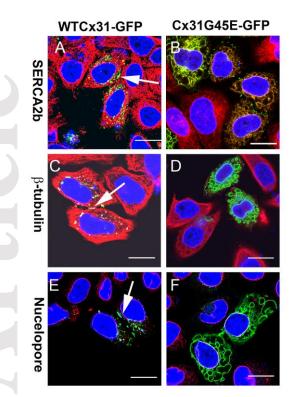
52.   Sugiura, K., Unfolded protein response in keratinocytes: impact on normal and abnormal keratinization. *J Dermatol Sci* **2013,** 69, (3), 181.

53.   Terasaki, M.; Chen, L. B.; Fujiwara, K., Microtubules and the endoplasmic reticulum are highly interdependent structures. *J Cell Biol* **1986,** 103, (4), 1557.

54.   Li, T. C.; Kuan, Y. H.; Ko, T. Y.; Li, C.; Yang, J. J., Mechanism of a novel missense mutation, p.V174M, of the human connexin31 (GJB3) in causing nonsyndromic hearing loss. *Biochem Cell Biol* **2014,** 92, (4), 251.

55. Richard G, Smith LE, Bailey RA, Itin P, Hohl D, Epstein EH, Jr., DiGiovanna JJ, Compton JG, Bale SJ (1998) Mutations in the human connexin gene GJB3 cause erythrokeratodermia variabilis. *Nature genetics* **20:** 366-369

56. Wilgoss A, Leigh IM, Barnes MR, Dopping-Hepenstal P, Eady RA, Walter JM, Kennedy CT, Kelsell DP (1999) Identification of a novel mutation R42P in the gap junction protein beta-3 associated with autosomal dominant erythrokeratoderma variabilis. *The Journal of investigative dermatology* **113:** 1119-1122

WTCx31-GFP   Cx31G45E-GFP

SERCA2b

β-tubulin

Nucelopore